

Dynamic analysis of ROV cable considering the coupling motion of ROV cable systems

Kyu Nam Cho[†]

*Department of Naval Architecture and Ocean Engineering, Hongik University,
Jochiwon, Chungnam 339-701, Korea*

Ha Cheol Song[‡]

*Research Institute of Marine Systems Engineering, Seoul National University, San 56-1,
Shillim-dong, Kwankak-gu, Seoul 152-744, Korea*

Do Chun Hong[‡]

*Korea Research Institute of Ships and Ocean Engineering, 171, Jang-dong,
Yusung-gu, Daejeon 305-343, Korea*

(Received December 4, 2003, Accepted July 14, 2004)

Abstract. Remotely Operated Vehicle of 6000-meters is a new conceptual equipment made to replace the manned systems for investigating the deep-sea environment, and all of the ROV systems in operational condition strongly depend on the connecting cables. In this point of view dynamics of the ROV cable system is very important for operational and safety aspects as a cable generally encounters great tension. Researches have been executed on this problem, and most of papers have been mainly focused on the operational condition of ROV system in deep sea. This paper presents the dynamic cable response analysis during ROV launching condition rather than the operational one in order to provide the design guide of a ROV cable system in this circumstance, considering the coupling effects between cable and wave-induced ship motion. To obtain the variations of cable tensions during a ROV launching, a pre-stressed harmonic response analysis was carried out. Wave-induced tensions of the cable during ROV launching were obtained in real sea states using FE modeling, and the basic design guide of a ROV cable system was obtained.

Key words: ROV cable system; coupling motion; dynamic cable response; pre-stressed harmonic response analysis; head and beam seas; significant wave.

1. Introduction

In the recent years, ROV has been developed to travel and approach an aimed object in deep sea and transmit some information of that to a support vessel by using tether cable (Cho and Yi 2002).

[†] Professor

[‡] Researcher

As the cable of ROV generally encounters great tension in deep sea due to hydrostatic and hydrodynamic forces in addition to gravity and inertia forces, most of preceding researches have been mainly focused on the assessment of dynamic behaviors of ROV-cable in this operational condition (Kawaguchi *et al.* 1999, Nagatomi *et al.* 2002). But it is another important problem to know cable dynamics in launching and recovery conditions for designing the cable and determining its safety.

In this point of view, this paper presents the dynamic cable response analysis during ROV launching condition rather than operational one, considering the coupling effects between a cable and a wave-induced ship motion.

To obtain the variations of cable tensions during a ROV launching, a pre-stressed harmonic response analysis was carried out. In this procedure, a static cable tension, induced by the weight of ROV and launching system, was considered first by performing the pre-stressed analysis before the harmonic response analysis. Wave-induced responses of support vessel were calculated with ship motion analysis in cases of head sea and beam sea states, consequently. Then the coupling effect was included in the calculation of the excitation forces of vibration analysis by introducing the concept of relative acceleration between cable and support vessel. Wave-induced tensions of the cable during ROV launching were obtained in real sea states using FE modeling, and the basic design guide of a ROV cable system was obtained.

2. Analysis of ship motion due to wave load

Onnuri, a specially purposed ship of KORDI (Korea Ocean Research and Development Institute), is adopted as a support vessel for the analysis of ship motion, and the principle dimensions of this vessel is listed in Table 1 (Cho 2002).

Table 1 Principle dimensions of 'Onnuri'

Length	63.6 m
Length (water plane)	55.5 m
Breadth	12.0 m
Depth	7.55 m
Draft	5.15 m
Speed	15.0 kts

2.1 Formulation of the problem (Hong *et al.* 1987)

The basic assumptions of formulation are as follows;

- Fluid is inviscid and incompressible.
- Fluid fills the volume, V , made up of free surface (\mathcal{F}), wetted surface of ship hull (S) and infinite water depth.

As to the coordinate system, the origin of the right-hand-sided Cartesian coordinate, O , is located on the waterline of ship hull. A $(x0y)$ plane corresponds to still water plane of the ship and the z -axis indicates the normal direction of this plane.

Fluid velocity can be obtained from velocity potential which satisfies the Laplace equation with the assumption of irrotational flow. If the incident wave (Airy wave) defined as velocity potential, ϕ_0 , comes from the infinite, velocity potentials can be obtained from incident potential, ψ_0 , as shown in Eqs. (1) and (2). The ship excited by an incident wave load has a characteristic of simple harmonic motion with infinitesimal amplitude, $O(\epsilon)$, and angular frequency, ω .

$$\phi_0 = \text{Re}\{\psi_0 e^{-i\omega t}\} \tag{1}$$

$$\psi_0 = -\frac{a_0 g}{\omega} e^{k_0[z + i(x\cos\beta + y\sin\beta)]} \tag{2}$$

- where, a_0 : infinitesimal amplitude
- ω : angular frequency
- g : gravitational acceleration
- k_0 : wave number ($= \omega^2/g$)
- β : wave direction from x -axis

Displacement of a point, M , on the surface, S , denoted by $\vec{A}(M)$ which has six degrees of freedom of floating body, is expressed as the following 3 equations. In these equations, M_0 and M_1 denote mean position and temporary position of the point, M .

$$\vec{A}(M) = \overrightarrow{M_0M_1} = \vec{a} + \vec{\theta} \times \overrightarrow{OM_0} \tag{3}$$

where, $\vec{a} = a_1\vec{e}_1 + a_2\vec{e}_2 + a_3\vec{e}_3$

$$\vec{\theta} = a_4\vec{e}_1 + a_5\vec{e}_2 + a_6\vec{e}_3 \tag{4}$$

$$a_j = \text{Re}\{\vec{a}_j e^{-i\omega t}\}, \quad j = 1, 2, \dots, 6 \tag{5}$$

The total potential, Ψ , of unsteady flow is obtained by a summation of three kinds of potentials: the incident potential, ψ_0 , the diffraction potential, Ψ_7 , and the radiation potential, Ψ_R (Eq. 6). As the incident potential is given, the derivation of diffraction potential and radiation potential are the kernel of this problem. When a floating body is rigid without inner free surface, it is well known that those potentials are obtained by solving 3-D radiation-diffraction problem in Eq. (7).

$$\Psi = \psi_0 + \Psi_7 + \Psi_R \tag{6}$$

$$\Psi_R = -i\omega \left\{ \sum_{k=1,2,6} a_k \psi_k + \sum_{k=3,4,5} a_k \psi_k \right\} \tag{7}$$

Diffraction potential, Ψ_7 in Eq. (6) and radiation potential, ψ_k ($k = 1, 2, \dots, 6$) in Eq. (7) should satisfy the radiation condition at infinity and the boundary conditions, as listed from Eq. (8) to Eq. (11), on free surface (F_0) and wetted surface (S_0). The subscript, o , appeared in \mathcal{F}_0 and S_0 describes the mean position of each surface.

$$\left(-k_0 + \frac{\partial}{\partial z}\right)\psi_k = 0 \quad \text{for } k = 1, 2, \dots, 7 \text{ on } \mathcal{F}_0 \quad (8)$$

$$\frac{\partial \psi_k}{\partial n_0} = \vec{e}_k \cdot \vec{n}_0 \quad \text{for } k = 1, 2, 3 \text{ on } S_0 \quad (9)$$

$$\frac{\partial \psi_k}{\partial n_0} = (\vec{e}_{k-3} \times \vec{OM}) \cdot \vec{n}_0 \quad \text{for } k = 4, 5, 6 \text{ on } S_0 \quad (10)$$

$$\frac{\partial \psi_k}{\partial n_0} = -\frac{\partial \psi_0}{\partial n_0} \quad \text{for } k = 7 \text{ on } S_0 \quad (11)$$

2.2 Potential solution from integration equation

Equations from (12) to (17) are obtained by applying Green's theorem to ψ_k ($k = 1, 2, \dots, 7$) and Kelvin-type Green function.

$$\begin{aligned} & \frac{\psi_k(P)}{2} - \iint_{S^i \cup S_c} \psi_k(M) \frac{\partial G_0(P, M)}{\partial n_M} ds - \iint_{F_0^i} \left[\psi_k(M) \frac{\partial G_0(P, M)}{\partial n_M} - k_0 \psi_k(M) G_0(P, M) \right] ds \\ & + \iint_{S_c} \frac{\partial \psi_k(M)}{\partial n_M} G_0(P, M) ds = - \iint_{S_i} \frac{\partial \psi_k(M)}{\partial n_M} G_0(P, M) ds, \quad P \text{ on } S^i \cup S_c \cup F_0^i \end{aligned} \quad (12)$$

$$G(P, M) = -\frac{1}{4\pi} \left\{ \frac{1}{\gamma(P, M)} + \frac{1}{\gamma'(P, M)} + [1 - \delta(z_P - 0) \cdot \delta(z_M - 0)] H(P, M) \right\} \quad (13)$$

$$\gamma'(P, M) = \frac{1}{[(x_P - x_M)^2 + (y_P - y_M)^2 + (z_P + z_M)^2]^{1/2}} \quad (14)$$

$$H(P, M) = \frac{2k_0}{\pi} \operatorname{Re} \int_{-\frac{\pi}{2}}^{+\frac{\pi}{2}} e^{\zeta} [J_1(\zeta) + i\pi] d\theta + 2ik_0 \operatorname{Re} \int_{-\frac{\pi}{2}}^{+\frac{\pi}{2}} e^{\zeta} d\theta \quad (15)$$

$$\begin{aligned} J_1(\zeta) &= E_1(\zeta), \quad \text{for } \operatorname{Im} \zeta > 0 \\ &= E_1(\zeta) - 2i\pi, \quad \text{for } \operatorname{Im} \zeta < 0 \end{aligned} \quad (16)$$

$$\zeta = k_0 \{ z_P + z_M + i[(x_P - x_M) \cos \theta + (y_P - y_M) \sin \theta] \} \quad (17)$$

In the above equations, \vec{n}_M is a normal vector at point, M , orienting fluid field from wetted surface, and $E_1(\zeta)$ is a complex exponential function. Through the discretization of these integration equations, solutions are derived from transformed linear algebraic equations.

2.3 Equations of motion

Fluctuating pressure acting on a wetted surface is derived from Bernoulli's equation of linearly

unsteady potential flow (Eq. (18)). It is widely known that the excitation force due to incident-diffraction potential, added mass and wave damping force due to radiation potential can be obtained by solving this equation. From the equilibrium conditions of force and moment acting on a floating body, the equation of motion is derived as Eq. (19). In this equation, m , Δ , I_{jk} , R_{jk} , M_{jk} , B_{jk} and F_j are correspond to mass, displacement, inertia coefficient, restoring force coefficient, wave damping coefficient and wave exciting force coefficient of a floating body, respectively, and D denotes the characteristic length of a structure.

$$p = -\rho \frac{\partial \Phi}{\partial t} = \rho \omega \text{Re}\{i\Psi e^{i\omega t}\} \tag{18}$$

$$\sum_{k=1}^6 [-\omega^2(mI_{jk} + \rho\Delta M_{jk}) - i\rho\Delta\omega^2 B_{jk} + \rho g D^2 R_{jk}] a_j = \rho a_0 \omega^2 D^3 F_j, \quad j = 1, 2, \dots, 6 \tag{19}$$

2.4 Estimation of significant number according to sea states

The amplitude of irregular wave, $a_0(\omega_i)$, that is wave energy, varies with the frequency of element wave, ω_i , and Eq. (20) shows this relation.

$$E_{\zeta_0} = \rho g \int_0^\infty S(\omega) d\omega = \frac{\rho g}{2} \sum_{i=1}^n a_0(\omega_i) \tag{20}$$

where, E_{ζ_0} , $S(\omega)$ and ρ represent the energy of irregular wave of unit length, wave spectrum and the density of fluid, respectively.

Even though many kinds of irregular wave spectrums have been reported, ITTC two-parameter wave spectrum of Pierson-Moskowitz type is used in this study (Eq. (21)). It is a narrow-banded wave spectrum, which is defined by significant wave height, $H_{1/3}$, and mean period, T_m .

$$S(\omega_0) = A \omega_0^{-5} \exp(-B \omega_0^{-4}) \tag{21}$$

where,

$$A = 173 \times \frac{H_{1/3}^2}{T_1^4}, \quad B = \frac{691}{T_1^4} \tag{22}$$

$$m_{\zeta_0} = \int_0^\infty S(\omega_0) d\omega_0 \tag{23}$$

$$H_{1/3} = 4\sqrt{m_{\zeta_0}} \tag{24}$$

2.5 Results of the analysis of ship motion

From the ship response derived from equations of motion and the wave spectrum, acceleration components at winch and top of A-frame due to wave load were obtained as listed from Table 2 to Table 5. Those results correspond to several cases of sea states; unit head sea and unit beam sea. The unit of acceleration is a dimensionless ratio which is a relative quantity compared to gravitational acceleration.

Table 2 Accelerations at winch; unit head sea (Unit: accel./gravitational accel.)

Frequency (Hz)	Acceleration in X		Acceleration in Y		Acceleration in Z	
	Re	Im	Re	Im	Re	Im
0.1	1.014E-03	-2.646E-05	9.447E-11	-1.206E-16	1.540E-05	1.019E-03
0.2	3.970E-03	-4.157E-04	3.493E-10	-1.817E-14	2.458E-04	4.065E-03
0.3	8.470E-03	-2.026E-03	7.696E-10	-1.023E-10	1.234E-03	9.045E-03
0.4	1.345E-02	-5.969E-03	1.265E-09	-1.688E-11	3.818E-03	1.560E-02
0.5	1.689E-02	-1.292E-02	1.557E-09	-6.979E-10	8.928E-03	2.285E-02
0.6	1.603E-02	-2.200E-02	9.639E-08	-2.110E-08	1.710E-02	2.920E-02
0.7	8.936E-03	-2.988E-02	3.414E-09	-2.024E-09	2.768E-02	3.241E-02
0.8	-3.069E-03	-3.141E-02	2.582E-09	-3.673E-09	3.798E-02	3.034E-02
0.9	-1.377E-02	-2.315E-02	1.741E-09	-4.337E-09	4.331E-02	2.258E-02
1.0	-1.530E-02	-8.334E-03	-4.140E-10	-4.336E-09	3.890E-02	1.243E-02

Table 3 Accelerations at A-Frame; unit head sea (Unit: accel./gravitational accel.)

Frequency (Hz)	Acceleration in X		Acceleration in Y		Acceleration in Z	
	Re	Im	Re	Im	Re	Im
0.1	1.010E-03	-2.645E-05	1.094E-10	-5.425E-16	-5.189E-06	1.019E-03
0.2	3.913E-03	-4.105E-04	3.718E-10	-1.716E-14	-8.250E-05	4.095E-03
0.3	8.187E-03	-1.964E-03	7.455E-10	-2.486E-11	-3.951E-04	9.400E-03
0.4	1.261E-02	-5.628E-03	1.219E-09	2.399E-10	-1.033E-03	1.757E-02
0.5	1.509E-02	-1.168E-02	1.582E-09	-3.611E-11	-1.419E-03	2.997E-02
0.6	1.321E-02	-1.866E-02	2.053E-07	-4.185E-08	8.408E-04	4.842E-02
0.7	6.036E-03	-2.282E-02	7.309E-09	-8.882E-10	1.096E-02	7.304E-02
0.8	-3.495E-03	-1.963E-02	6.862E-09	-4.787E-09	3.553E-02	9.822E-02
0.9	-8.195E-03	-8.130E-03	6.642E-09	-7.761E-09	7.545E-02	1.091E-01
1.0	-2.095E-03	4.576E-03	1.998E-09	-9.686E-09	1.150E-01	8.682E-02

Table 4 Accelerations at winch; unit beam sea (Unit: accel./gravitational accel.)

Frequency (Hz)	Acceleration in X		Acceleration in Y		Acceleration in Z	
	Re	Im	Re	Im	Re	Im
0.1	-1.123E-08	-4.585E-08	-1.013E-03	6.888E-11	6.911E-07	1.019E-03
0.2	-8.171E-08	-6.266E-07	-3.968E-03	8.426E-10	1.194E-05	4.077E-03
0.3	-1.854E-07	-2.993E-06	-8.576E-03	4.836E-08	7.011E-05	9.175E-03
0.4	1.705E-07	-1.001E-05	-1.411E-02	5.549E-07	2.897E-04	1.632E-02
0.5	5.385E-06	-2.624E-05	-1.779E-02	-1.655E-06	1.232E-03	2.555E-02
0.6	-1.924E-03	-7.493E-06	-9.527E-01	4.131E-02	-2.100E-01	4.520E-02
0.7	-5.523E-05	-1.210E-04	-5.624E-02	5.681E-04	-3.614E-03	5.069E-02
0.8	-8.286E-05	-2.351E-04	-6.103E-02	1.282E-03	-3.158E-03	6.712E-02
0.9	-1.730E-04	-4.712E-04	-6.817E-02	2.891E-03	-4.447E-03	8.688E-02
1.0	-3.324E-04	-1.017E-03	-7.484E-02	5.868E-03	-8.829E-03	1.109E-01

Table 5 Accelerations at A-Frame; unit beam sea (Unit: accel./gravitational accel.)

Frequency (Hz)	Acceleration in X		Acceleration in Y		Acceleration in Z	
	Re	Im	Re	Im	Re	Im
0.1	-2.926E-08	-1.219E-07	-1.009E-03	-1.963E-11	1.797E-06	1.019E-03
0.2	-2.123E-07	-9.749E-07	-3.902E-03	4.761E-10	3.105E-05	4.075E-03
0.3	-4.751E-07	-4.177E-06	-8.201E-03	3.468E-08	1.823E-04	9.168E-03
0.4	5.113E-07	-1.406E-05	-1.259E-02	2.357E-07	7.536E-04	1.630E-02
0.5	1.446E-05	-3.927E-05	-1.146E-02	-6.653E-06	3.211E-03	2.547E-02
0.6	-5.000E-03	3.703E-05	-2.000E+00	8.325E-02	-5.460E-01	5.819E-02
0.7	-1.295E-04	-2.251E-04	-7.293E-02	7.456E-04	-9.114E-03	5.014E-02
0.8	-1.463E-04	-4.946E-04	-7.254E-02	1.634E-03	-7.019E-03	6.573E-02
0.9	-1.771E-04	-1.077E-03	-7.772E-02	3.738E-03	-7.372E-03	8.364E-02
1.0	-5.713E-05	-2.309E-03	-8.286E-02	7.789E-03	-9.679E-03	1.041E-01

3. Dynamic response analysis with the coupled motion of support vessel

3.1 Formulation of the problem

Generally, a ROV cable system is composed of cable, ROV, launcher and support vessel with A-frame. The dynamics of each system can be represented by the following set of equations. Where, the matrices, $[M]$, $[C]$, $[K]$ and $\{F(t)\}$, correspond to mass, damping, stiffness and external force of each system, and subscripts, s , a and c denote support vessel, A-frame and cable, respectively.

$$[M_s]\{\ddot{x}_s(t)\} + [C_s]\{\dot{x}_s(t)\} + [K_s]\{x_s(t)\} = \{F_s(t)\} \tag{25}$$

$$[M_a]\{\ddot{x}_a(t)\} + [C_a]\{\dot{x}_a(t)\} + [K_a]\{x_a(t)\} = \{F_a(t)\} \tag{26}$$

$$[M_c]\{\ddot{x}_c(t)\} + [C_c]\{\dot{x}_c(t)\} + [K_c]\{x_c(t)\} = \{F_c(t)\} \tag{27}$$

Scrutinizing the previous researches on the dynamic analysis of coupled motion, the most popular approach for solving this problem is to impose the coupled effects of each system on the other system. Corresponding to this approach, all the excitation forces of support vessel and A-frame which may affect the dynamic behavior of cable were transformed to the excitation force of cable. In Eq. (28), F_0 is the amplitude of excitation force of cable, which has the coupling effect of ship motion. The procedure for the derivation of F_0 is mentioned below in detail.

$$[M_c]\{\ddot{x}_c(t)\} + [C_c]\{\dot{x}_c(t)\} + [K_c]\{x_c(t)\} = \{F_0 \sin \omega t\} \tag{28}$$

3.2 Assessment of harmonic excitation force of cable

To estimate cable excitation forces induced by ship motion, authors would like to propose the concept of relative acceleration considering the geometry of support vessel. The proposed procedure is as follows.

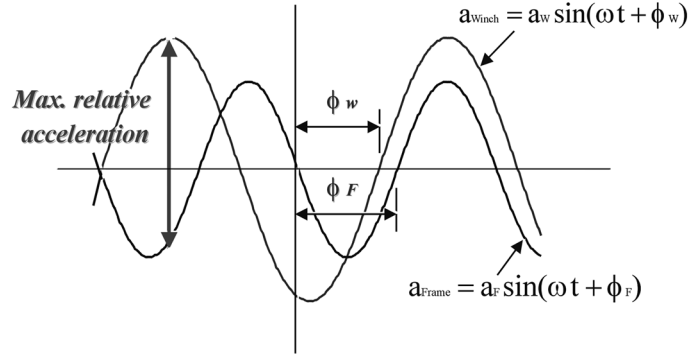


Fig. 1 Max. relative acceleration between winch and A-frame

- Winch of support vessel is assumed to be fixed.
- As shown in Fig. 1, the maximum amplitude of relative acceleration between winch and the top of A-frame can be obtained from the results of ship motion analysis by considering the phase difference of acceleration components.
- Finally, the amplitude of cable excitation forces is estimated by multiplying maximum relative acceleration by the summed mass of ROV and launcher.

Table 6 and Table 7 show the cable excitation forces obtained from the above procedure in the cases of head sea and beam sea, which have unit amplitude.

$$\begin{aligned} \vec{a} &= \text{Re} + i\text{Im} \\ &= \sqrt{\text{Re}^2 + \text{Im}^2} \sin(\omega t + \phi) \end{aligned} \tag{29}$$

where,

$$\phi = \tan^{-1} \frac{\text{Im}}{\text{Re}}$$

$$\text{relative acceleration} = a_w \sin(\omega t + \phi_w) + a_f \sin(\omega t + \phi_f) \tag{30}$$

Table 6 Cable excitation force in unit head sea

Freq. (Hz)	F _x (N)	F _y (N)	F _z (N)
0.10	-0.2	0.0	89.9
0.20	-2.5	0.0	360.0
0.30	-12.8	0.0	814.4
0.40	-40.1	0.0	1468.0
0.50	-96.2	0.0	2353.4
0.60	-192.7	0.0	-1110.4
0.70	-336.3	0.0	-1938.1
0.80	519.9	0.0	-2995.8
0.90	706.7	0.0	-4072.1
1.00	814.6	0.0	-4694.1

Table 7 Cable excitation force in unit beam sea

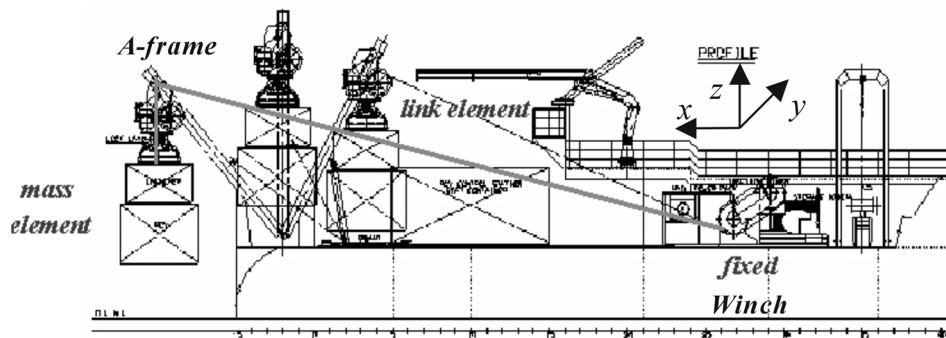
Freq. (Hz)	F _x (N)	F _y (N)	F _z (N)
0.10	0.0	-0.2	0.1
0.20	0.0	-2.9	0.8
0.30	-0.1	-16.5	5.0
0.40	0.2	-67.1	20.5
0.50	0.7	-279.6	87.3
0.60	135.7	46243.0	14831.2
0.70	-5.6	736.4	-243.8
0.80	-11.8	507.8	-181.0
0.90	-26.7	422.8	-192.3
1.00	-58.3	363.8	-304.9

3.3 Pre-stressed harmonic response analysis

To assess the dynamic behaviors of cable due to wave load, harmonic response analysis was carried out in this study considering the geometric information of ‘Onnuri’ as a support vessel. As shown in Fig. 2, cable, ROV, and launcher were modeled by using link element and mass element, respectively (Chung and Cheng 2002). Referring to the existing tether cable, ROV, and launcher, material properties of finite elements used in this analysis were adopted as listed in Table 8, and ANSYS was used as a solver (ANSYS 5.7).

Especially, before harmonic response analysis, pre-stress analysis was performed to impose static tension, due to the weight of ROV and launcher on cable, since it has been known that the pre-existing tension greatly affects the dynamic behavior of cable.

As a boundary condition, the position of winch was maintained fixed on the basis of the assumption for obtaining relative acceleration, as mentioned above.



Longitudinal distance from winch to top pf A-frame : 39.235 m
 Height of top of A-frame from deck during launching : 7.787 m

Fig. 2 Finite element modeling of ROV cable system

Table 8 Material properties of finite element

Element type	Items	Value
Link8	Stiffness (EA)	9.79×10^3 kN
	density	4428.75 kg/m ³
Mass21	mass	4000 kg

4. Results of harmonic responses and discussions

Fig. 3 and Fig. 4 show the results of pre-stressed harmonic response analysis of the cable. These results are cable tensions induced by various sea states; head sea and beam sea, 1 m and 3 m in wave amplitude. The assessed frequency range of wave is from 0.1 Hz to 1.0 Hz since most of significant waves in ocean have its own frequency in this region.

As a result of Fig. 3, maximum cable tension is evaluated as 1.5 ton under the condition of head sea and 1 Hz, the wave frequency. Even if this cable tension is added to static cable tension, 5 ton, due to the gravitational force of ROV and launcher, the summed value, 6.5 ton, is relatively small compared to the tensile strength of cable, 17 ton. So it is concluded that the designed cable has sufficient safety margin in head sea state.

But, in beam sea state, a more detailed verification about resonance is needed before the final design of cable since the possibility of resonance is noticed from the analysis results, near 0.6 Hz in wave frequency, as shown in Fig. 4.

The authors are now going to go further researches for the assessment of cable tension considering other influence parameters; changes of cable length during launching, braking operation and environmental load in severe sea state.

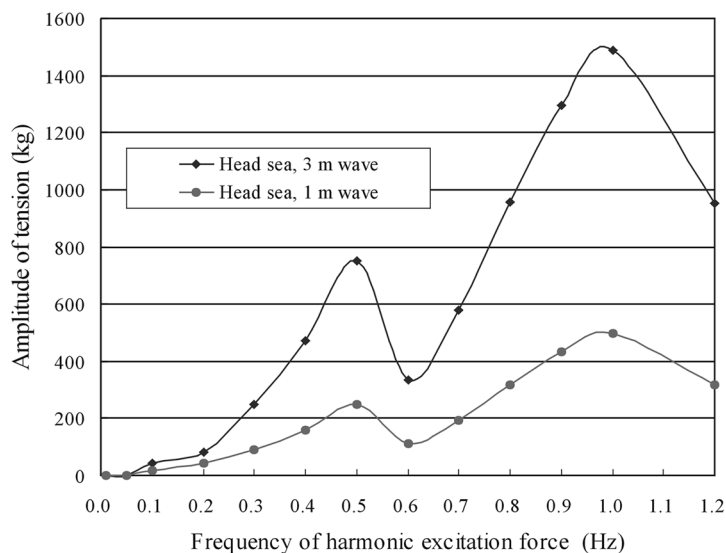
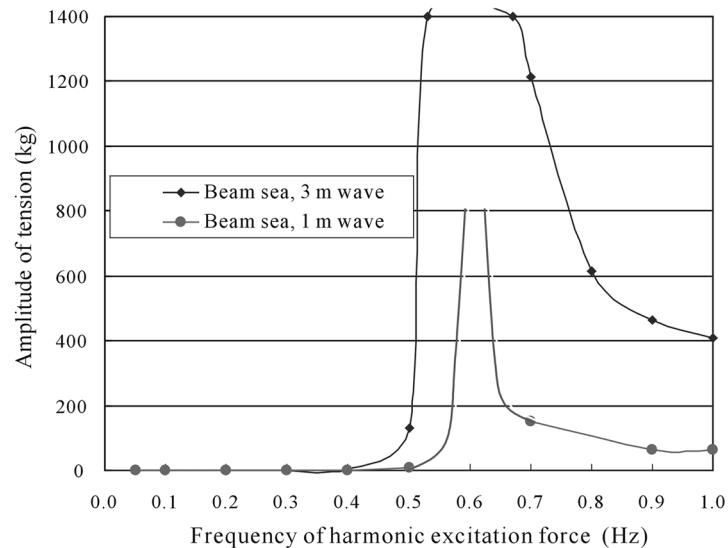


Fig. 3 Harmonic response of cable tension due to head sea



<Note> Cable tension at 0.6 Hz : 404,032 kg for 1 m wave
2,124,113 kg for 3 m wave

Fig. 4 Harmonic response of cable tension due to beam sea

5. Conclusions

In this paper, the dynamic cable response analysis during ROV launching condition was carried out considering the coupling effects between cable and wave-induced ship motion; thus following conclusions were drawn.

- The analysis of wave-induced ship motion was carried out for an existing support vessel according to sea states, and the coupling effect between cable and ship motion was included in the calculation of the excitation forces of vibration analysis by introducing the concept of relative acceleration.
- To consider the effect of static cable tension induced by the weight of ROV and launching system, in this study, pre-stressed harmonic response analysis was proposed to obtain the variations of cable tensions during ROV launching.
- In head sea state with 3m amplitude, maximum variation of cable tension is evaluated relatively small compared to tensile strength of cable, 10% of tensile strength, so it can be concluded that the cable is almost safe in this environment. But, in beam sea state, it is noticed that a resonance may occur in specific excitation frequency.

References

ANSYS 5.7, User's Guide.

Cho, K.N. (2002), "A study on the design of A-frame and Devices for Deep-Sea ROV and AUV", Technical Report, Hong-ik University.

Cho, K.N. and Yi, W.S. (2002), "Development of a dynamic analysis scheme of cable for ROV operation", *Proc.*

- of Twelfth Int. Offshore and Polar Eng. Conf.*, Kitakushu, Japan.
- Chung, J.S. and Cheng, B. (1999), "3-D responses of vertical pipe bottom pin-jointed to a horizontal pipe to ship motion and thrust on pipe - Part I: MSE and FEM modeling", *Proc. of Ninth Int. Offshore and Polar Eng. Conf.*, Brest, France.
- Hong, D.C., Hong, S.Y. and Lee, S.M. (1987), "On the wave loads on a large volume offshore structure", *J. Ocean Eng. and Tech.*, **1**(1).
- Kawaguchi, K., Iwase, R. and Momma, H. (1999), "Underwater operation for complex deep seafloor observatory using demission submarine cable", *Proc. of Ninth Int. Offshore and Polar Eng. Conf.*, Brest, France.
- Nagatomi, O., Nakamura, M. and Koterayama, W. (2002), "Dynamic simulation and field experience of submarine cable during laying and recovery", *Proc. of Twelfth Int. Offshore and Polar Eng. Conf.*, Kitakushu, Japan.